Discovery of Bioactive Compounds From Medicinal Plants: Insights Into *Wrightia Tinctoria* as a Potential Antistaphylococcal Agent Targeting

Vidya S L
Kongunadu Arts and Science College
Anantha Bhairavi
Kongunadu Arts and Science College
R Sathishkumar
rsathishkumar_bt@kongunaducollege.ac.in

Kongunadu Arts and Science College

Research Article

Keywords: Staphylococcus aureus, Drug resistantance, Phytocompounds, Wrightia tictoria, Molecular Docking, Dynamic simulations, Antibaterial analysis

Posted Date: May 7th, 2025

DOI: https://doi.org/10.21203/rs.3.rs-6232250/v1

Additional Declarations: No competing interests reported.

Version of Record: A version of this preprint was published at In Silico Pharmacology on February 4th, 2026. See the published version at https://doi.org/10.1007/s40203-025-00545-9.

Abstract

Staphylococcus aureus,a prominent pathogen demonstrate robust survival capabilities both within and outside host cells.The alarming rise of antibiotic resistance strains poses substantial challenge in modern medicine.Bioactive compounds from medicinal plants could be an effective alternative due to their presence of diverse secondary metabolites. The present study aim to conduct insilico docking and dynamic simulations to identifypromising bioactive compound from medicinal plants against virulence protein Clumping factor A of *Staphylococcus aureus* through bioinformatic approach. Initial ADME screening of phytocompounds from the plants *Breynia retusa*, *Hemigraphis alternata*, *Imperata cylindrica*, *Oldenlandia corymbosa*, *Sida rhombifolia*, *Scoparia dulcis*, *Tephrosia purpurea* and *Wrightia tinctoria* R were conducted to comprehend their pharmacokinetic profile, followed by docking and dynamic simulations.As a result, indirubin showed effecient binding interaction with target protein, offering remarkable G score value of -8.82 Kcal/Mol. In addition, dynamic stimulations validated the top docked complex with significant RMSD and RG stability besides desirable binding free energy in contrast to the standard drug neomycin sulphate. To validate these results, the antibacterial potential of the fresh and dry leaf extract of *Wrightia tinctoria* was tested, showing strong inhibitory effects against *Staphylococcus aureus* with a maximum zone of inhibition of 26.33 ± 0.33 mm. A detailed analysis of the ethyl acetate extract using GC-MS revealed the presence of 50 bioactive compounds, underscoring the plant's potential as a natural antimicrobial source. These outcomes indicate that *W. tinctoria* holds promise as a therapeutic option for managing staphylococcal infections and highlights the need for further research to explore its clinical applications.

INTRODUCTION

Staphylococcus aureus, a Gram-positive bacterium, is one of the most prevalent bacterial species identified in chronic wounds and various other bacterial infections. The pathogen is implicated in both community-based and hospital-acquired infections; however, the treatment is exceedingly challenging due to the prevalence of multidrug-resistant strains (Roy *et al.*, 2020; Hasan et al., 2016). The World Health Organization (WHO) considers antimicrobial resistance as a prime threat to global health and enlists the bacterial priority pathogens and strategies to prevent the resistance (WHO, 2024). Reports unveiled that around 50% of infectious bacteria like *E. coli*, *K. pneumoniae*, *S. aureus*, and *P. aeruginosa* exhibit resistance to some of the most effective antibiotics, including third-generation cephalosporins (Tillotson and Zinner 2017; Terreniet al., 2021). Studies have been considered to reduce the rate of microbial infections and promote appropriate usage of active antimicrobial drugs. Several virulence factors, including enterotoxins, toxins, hemolysins (alpha, beta, gamma, and delta), metalloprotease, and hyaluronidase as well as biofilm formation renders a major role in the multidrug resistance mechanisms. The coaggregation of free-floating microbes into multiple layers in biofilm is often facilitated by adhesion via cell wall proteins(He et al., 2024). Clumping factor A (ClfA) is a cell-wall anchored protein of *S. aureus* actively involved in adhesion facilitated by existing sheer mechanical tension through fibrinogen binding(Herman-Bausieret al., 2018). This virulence protein initiates infections by inhibiting phagocytosis with enhanced efficacy in the presence of fibrinogen, highlighting its role in *S. aureus*

immune evasion (Higgins et al., 2006). Altogether these strategies contribute to the persistent susceptibility to *S. aureus* infections throughout an individual's lifetime (Bhattacharya and Horswill, 2024). Therefore, the present study focuses on utilizing this crucial virulence factor of *S. aureus* as a target for drug designing purposes.

Phytomedicines have played a crucial role in traditional healthcare systems worldwide for millennia entailed with fewer adverse side effects (Yuan et al., 2016). Despite the extensive literature available on therapeutic properties, standardized procedures for their identification, phytochemical analysis and pharmacological evaluation are scarce (Patel et al., 2012; Thakur et al., 2020).Recent studies desperately highlighted the propitious antimicrobial activity of phytocompounds in averting the resistance mechanisms of ESKAPE pathogens which includes*Enterococcus faecium, Staphylococcus aureus, Klebsiella pneumoniae, Acinetobacter baumannii, Pseudomonas aeruginosa*, and *Enterobacter species*(Bhatia et al., 2021; Ashhar *et al.*, 2024).With this perspective, the secondary metabolites of the following plants *Breynia retusa*, *Hemigraphis alternata, Imperata cylindrica, Oldentia corymbosa*, *Sida rhombifolia*, *Scoparia dulcis, Tephrosia purpurea*, and *Wrightia tinctoria* were chosen to study its binding efficiency with clumping factor ClfA of *S. aureus*.

In the exploration of promising plant derived antibiotics, bioinformatics plays an indispensable role by facilitating the identification and validation of potential drug targets through high throughput screening. Thus, allows bioactive compounds from plants to be analyzed for their underlying molecular mechanism with the target protein (Szymański*et al.*, 2012; Babar *et al.*,2017; Mitra et al., 2022). The present study utilizes molecular docking, ADME (Adsorption, Distribution, Metabolism, Excretion) profiling, biological activity prediction and molecular dynamics approaches to identify the most promising drug candidate from the assorted medicinal plants. Additionally, antibacterial screening was conducted to validate in silico findings, followed by GC-MS analysis to identify and characterize the bioactive compounds present in the most effective extract. This extensive approach highlights viable options for preventing staphylococcal infections by bridging the gap between computational predictions and experimental confirmation.

MATERIALS AND METHODS

PROTEIN RETRIEVAL AND ACTIVE SITE PREDICTION

Protein data bank was used to retrieve the 3-dimensional structure of target protein clumping factor A (ClfA) PDB ID: 2VR3) from RCSB Protein Data Bank(www.rcsb.org) (Prlićet al., 2016). Followed by active site prediction using SCFBio online web tool (http://www.scfbio-iitd.res.in/dock/ActiveSite.jsp) pocket (Moulishankar and Sundarrajan 2024).

LIGAND RETRIEVAL AND PREPARATION

The 2D structure of literature proven secondary from the following assorted plants *Breynia retusa*, *Hemigraphis alternata, Imperata cylindrica, Oldentia corymbosa*, *Sida rhombifolia*, *Scoparia dulcis, Tephrosia purpurea*, and *Wrightia tinctoria*, were retrieved from the PubChem database together with their respective PubChem ID (https://pubchem.ncbi.nlm.nih.gov/) (Sasikumar *et al.*, 2022). Lig prep module of Maestro Schrodinger suite was utilized to prepare the ligands. Which includes enumeration of their all possible protonation and ionization states using Ionizer at a pH of 7.4 by addition or removal of protons from the ligand(Sahayarayan et al., 2021).

ADME PREDICTION

Around 105 assorted phytocompounds were screened for Adsorption, Distribution, Metabolism and Excretion (ADME) profiling using QikProp module of Schrodinger software to comprehend their pharmacokinetic properties in compliance with Lipinski's rule of five. Enlisting parameters like drug likeliness of small molecules with rotatable bonds, molecular weight, dipole moment, hydrogen bond donor and blood barrier coefficient being the prime parameters (Bhairavi et al., 2023; Patidar et al., 2019).

BIOLOGICAL ACTIVITY PREDICTION

The only compounds, obeys Lipinski’s rule of five are solely considered for their biological activity prediction using an online tool PASS (Prediction of Activity Spectra for Substances) way2drug (http://www.way2drug.com/passonline/predict.php) (Yusofand Segall 2013; Filimonovet al., 2014)

MOLECULAR DOCKING

ADME cleared compounds were used to perform docking analysis. GLIDE module in maestro Schrödinger software http://www.schrodinger.com/ was widely used to perform docking analysis (Bhairavi et al., 2023). It identifies potential areas of interaction between ligands and proteins by using a hierarchical series of filters that identifies the precise site of the ligand within the active site of the protein (Sahayarayanet al., 2021).The interactions of each compound with significant Glide score were visualized using the software PyMol (Mishra et al., 2021).

MOLECULAR DYNAMIC SIMULATIONS

To explore the protein-ligand interaction, the best docked compound was subjected to MD simulations along with standard compound Neomycin sulphate. Gromacs 2019.4 software suite was employed to analyze its interactions at atomic level (Cardoza et al., 2024). The energy-minimized protein-ligand complex was placed in a vacuum and solvated using the SPC water box and then equilibrated under NPT conditions. A 100 ns production run at constant temperature and pressure followed this step (Gangadharappa et al., 2020). RMSD, RMSF, Rg, SASA, and hydrogen bond interactions were evaluated

with trajectory analysis by Prasanth *et al*. Binding free energy, ΔG binding, was calculated using the MM-PBSA method with the g_mmpbsa tool, and energy decomposition for the last 50 ns of the trajectory gave insights into binding stability and affinity (Wang et al., 2019; Prasanth et al., 2021).

SAMPLE COLLECTION AND EXTRACTION

The sample *Wrightia tinctoria* was collected and authenticated *(BSI/SRC/5/23/2023-24/Tech/529)* from The Botanical Survey of India (BSI) Coimbatore, Tamilnadu.The parts including leaf, bark, and seeds were washed, shade-dried, and finely powdered. Fifty grams of sample (fresh and dried) used for extraction via maceration in 1:10 ratio for seven days, following Haile *et al.* (2022). The extracts were filtered with Whatman No. 1 paper, and the solvents (n-hexane, ethyl acetate and methanol) were evaporated under reduced pressure using a rotary evaporator. The resulting extracts were stored for subsequent analyses.

ANTIBACTERIAL SCREENING

Agar well diffusion method was carried out to evaluate the antibacterial efficacy of *W. tinctoria* (Jegadeeshwari et al., 2023). Extracts from fresh and dry plant materials in n-hexane, ethyl acetate, and methanol were studied against *Staphylococcus aureus* (MTCC-96). An overnight culture of *S. aureus*, with optical density was adjusted to 0.1, was inoculated on Muller Hinton Agar plates.6 mm wells were prepared and charged with 100µl of plant extracts at a concentration of 1ml/ml. Neomycin sulphate was considered as positive control and organic solvents were used as negative control. Further plates were incubated at 37°C for 24 hrs.

ANTIBIOTIC SUSCEPTIBILITY STUDIES

Kirby-Bauer disc diffusion method was used to analyse antibiotic susceptibility (Kirby and Bauer, 1966). Muller Hinton agar plates were evenly swabbed with S. aureus that was adjusted to 0.5 McFarland standard. Antibiotic disks (Himedia) including Azithromycin (AZM15), Methicillin (MET5), Streptomycin (S10), Vancomycin (VA30), Tetracycline (TE30), Colistin (CL10), Imipenem (IP8), and Piperacillin (PI100), were used with four discs placed on each plate.

For neomycin sulphate, antibiotic susceptibility was assessed using the agar well diffusion method, with 50 µg of neomycin sulphate per well. subsequently plates were then incubated overnight at 37°C, and the results were recorded.

GC-MS ANALYSIS

Phytochemical profiling of the ethyl acetate extract of *Wrightia tinctoria* was conducted using GC-MS analysis (GC-MS-QP 2010, Shimadzu, Tokyo, Japan). The analysis utilized an electron ionization energy of 70eV. A standard, non-polar 60 M TRX 5-MS column with dimensions of 30 m in length and a film thickness of 0.25 µm was employed. The instrument's oven temperature was programmed to increase

from 100°C to 260°C at a rate of 10°C per minute. Helium was used as the carrier gas, and 2 µl of the sample was injected initially at a steady flow rate of 2 ml per minute. With peak normalisation, the GC-MS analysis proceeded for thirty-five minutes. The identification of several components was made easier by this study. The National Institute of Standards and Technology (NIST) Mass Spectral Library version 2.0 (2005) mass spectra database was used in order to interpret the results (Khan et al., 2021).

RESULTS

ACTIVE SITE PREDICTION

2D image of target protein ClfA was shown in Fig. 1. The chosen X-ray crystallographic structure is characterized with chain A and B comprises of a sequence length of 329 residues. The Among the several cavities, the active site was predicted in cavity 1 that represents the following amino acid residues were predicted as their active site binding pocket: 16 SER, 17 GLY, 18 THR, 19 THR, 21 TYR, 22 PRO, 24 GLN, 25 ALA, 26 GLY, 27 TYR, 28 VAL, 29 LYS, 58 GLY, 59 VAL, 106 TYR, 107 ILE, 109 PRO, 115 THR, 134 LEU, 136 ASP, 137 TYR, 138 GLU, 139 LYS, 140 TYR, 141 GLY, 142 LYS, 150 GLY, 153 ASP, 164 GLN, 166 ILE, 167 TYR, 184 LEU, 185 LYS, 186 PRO, 187 ASN, 188 THR, 190 SER, 20 VAL, 225 GLY, 215 SER, 251 PRO, 252 HIS, 254 ALA, 258 ALA, 264 GLY, 265 ASP, 267 ALA, 269 ARG, 271 THR, 284 MET, 286 ASN, 287 GLY, 288 VAL, 289 GLU, 291 ALA, 292 PHE, 293 LYS, 295 LEU, 316 THR, 317 ASN, 318 VAL, 319 THR, 320 VAL, 321 GLY, 322 ILE, 323 ASP, 324 SER, 326 THR, 338 TYR. 339 ILE, 339 ASP, 357 THR, 384 ILE, 395 ARG, 430 THR, 432 ALA, 433 THR, 434 GLY, 435 ILE, 436 GLY, 437 SER, 438 THR, 439 THR, 440 ALA, 441 ASN, 442 LYS, 443 THR, 444 VAL, 525 ASN, 526 GLU, 532 GLY622 LEU, 623 GLY, 625 ALA, 624 GLY, 626 LYS, 627 GLN.

PREDICTION OF ADME PROPERTIES AND PHARMACOLOGICAL ACTIVITIES

The secondary metabolites of the plants *Breynia retusa, Hemigraphis alternata, Imperata cylindrica, Oldentia corymbosa*, *Sida rhombifolia*, *Scoparia dulcis, Tephrosia purpurea*, and *Wrightia tinctoria*, are collected and analyzed for ADME properties. Out of 78 compounds only 19 compounds cleared Lipinski's rule of five along with molecular weight, hydrogen donor and acceptor, logP value, various other factors like permeability for blood/brain barrier and skin, dipolar property, polar surface area, ionization potential, polarizability, electron affinity, number of rotatable bonds (Table 1).

Further, pharmacological activity of these 19 compounds were predicted through PASS online Way2Drug web tool where the importance was given to antibacterial activity. Almost all the compounds listed had antibacterial activity, except 17beta-Hydroxy-28-norolean-12-ene-3,16-dione. However, this compound was predicted to possess wound healing properties. Since each compound is predicted with significant and expected antibacterial activity, all the compounds were considered for molecular docking analysis.

DOCKING ANALYSIS

Molecular docking interactions for all the 19 compounds were conducted, however, 15 of the compounds had significant interactions with the amino acid residues of ClfA. The substantial Glide score (Kcal/mol), interacting residues, number of hydrogen bonds along with their bond length (Å) are tabulated (Table 2). The top docked compound Indirubin, had highest glide score of -8.82Kcal/mol forming four hydrogen bonds with active site residues GLY 225 and ILE339. The standard drug used was neomycin sulfate, which exhibited a G score of -8.45 kcal/mol. The second-best docked compound Indigo had a G score of -7.19 indicating strong binding interactions with key amino acid residues in active site pocket. The remaining compounds had a glide score ranging from – 6.77 to -2.93Kcal/mol. Amino acid interaction of all these compounds along with standard drug was tabulated in table and their interactions with clumping factor A (ClfA: 2VR3) are visualized using PyMol software (Fig. 1).

Table 2
Protein- Ligand Interaction Profile for the selected phytocompounds against target protein Clumping factor ClfA

S.No	Name of the Ligand (PubChem ID)	Residues Interaction	Bond Length (Å)	No. of Hydrogen Bonds	G-Score (Kcal/Mol)
Wrightia tinctoria					
1	Indirubin (10177)	GLY 225 (O-O)	2.9	4	-8.82
		ILE 339 (O-H)	2.6		
		ILE 339 (O-H)	1.9		
		ILE 339 (O-H)	2.3		
2	Indigo (10215)	PRO 251 (H-O)	2.2	4	-7.19
		ASN 525 (O-H)	2.3		
		ILE 384 (O-H)	1.9		
		ILE 384 (H-O)	1.9		
3	Palmitic acid (985)	ILE 384 (O-H)	1.8	3	-6.77
		ASN 525 (O-H)	1.6		
		GLU 526 (O-H)	2.6		
4	Isatin (7054)	GLY 255 (H-O)	1.9	2	-5.95
		VAL 288 (O-H)	2.1		
5	Phytol (5280435)	GLY 287 (H-O)	1.8	1	-5.67
6	Diethyl phthalate (6781)	HIS 252 (O-H)	2.1	1	-4.95
7	Urs-12-en-3beta-ol (225688)	GLY 287 (H-O)	2.0	1	-3.39
8	Ursolic acid (64945)	ARG 395 (O-H)	2.1	1	-2.93
Sida rhombifolia					
9	Vasicinol (442934)	ALA 258 (H-O)	2.4	2	-5.25
		ILE 339 (H-O)	1.9		
Tephrosia purpurea					
10	Purpurin (6683)	ILE 384 (H-O)	2.1	2	-4.92
		ILE 339 (H-O)	2.0		
11	Semiglabrin (156341)	ILE 384 (O-H)	2.4	3	-4.86

S.No	Name of the Ligand (PubChem ID)	Residues Interaction	Bond Length (Å)	No. of Hydrogen Bonds	G-Score (Kcal/Mol)
Wrightia tinctoria					
		ALA 254 (O-H)	2.3		
		ILE 339 (O-O)	2.8		
Scoparia dulcis					
12	5- Benzyloxypyrimidine (561874)	ILE 384 (N-H)	2.6	4	-4.84
		ILE 384 (O-H)	2.2		
		ASN525 (O-H)	2.3		
		ASN 525 (O-H)	2.0		
13	Benzofuran 2,3 dihydro (20209882)	TYR 338 (O-H)	2.2	4	-4.66
		LEU 295 (H-O)	2.4		
		LYS 293 (H-O)	2.6		
		GLY 532 (O-H)	2.3		
Breynia retusa					
14	Epicatechin (72276)	ILE 339 (H-O)	2.2	5	-4.75
		PRO 251 (H-O)	1.9		
		GLU 526 (H-O)	1.8		
		GLU 526 (O-H)	1.9		
		TRP 523 (O-H)	2.5		
Standard Antibiotic					
15	Neomycin sulphate (8378)	ASN 286 (O-H)	2.0	6	-8. 45
		ASP 385 (H-O)	1.8		
		GLU 342 (H-O)	1.8		
		GLU 342 (H-O)	1.8		
		ASP 340 (H-O)	2.1		
		LEU 283 (H-O)	2.2		

MOLECULAR DYNAMICS SIMULATION

Molecular dynamics simulation analysis is performed for the best interaction recorded in the docking analysis together with the standard drug interaction for 100 ns of. The changes in the protein-ligand complexes are accounted with the parameters such as root mean square deviation (RMSD), root mean square fluctuation (RMSF), the radius of gyration (Rg), hydrogen bond (H-bond), solvent accessible surface area (SASA), and further binding free energy (ΔGbind) was computed using the 'g_mmpbsa tool'.

RMSD AND RMSF

The calculation of RMSD describes the dynamic stability of a protein's backbone framework over the course of the simulation. The RMSD value and the trajectories were observed for 100 ns as shown in the figure (Fig. 2, Fig. 3). The receptor-ligand complexes: ClfA-indirubin and ClfA-neomycin sulphate as well as the ligands separately are simulated. The RMSD values for a period of 100 ns for the Indirubin and Neomycin Sulphate protein complexes were measured and found to be 0.18 +/- 0.035 nm and 0.29 +/- 0.069 nm, respectively. These results suggest minimal structural changes in the protein complexes during the simulation, with RMSD values that did not significantly differ from those of the unbound protein. These findings indicate the compounds' relative stability throughout the simulation. Overall, the protein complexes remained relatively stable throughout the simulation, with only minor differences between them, suggesting their similarity in terms of stability.

During a 100 ns simulation, the RMSF (root mean square fluctuation) was calculated to understand how the protein's vibrations change over time. This analysis provides insight into the movements of amino acids throughout the MD run and can determine how the absence or presence of a ligand affects protein stability. Figure 4 displays the RMSF results for the Indirubin and Neomycin Sulphate complexes. Based on these results, it appears that there were no significant structural changes throughout the simulation.

RADIUS OF GYRATION:

The radius of gyration (Rg) measuresthe compact a protein's structure (overall shape and folding changes) via the Rg plot. Both the Indirubin and Neomycin Sulphate complexes had similar Rg values. The average Rg value for the Indirubin and Neomycin Sulphate protein complexes from 0 to 100 ns were 2.36+/-0.014 nm and 2.45+/-0.019 nm respectively. Figure 5shows the Rg plot for both indirubin (black) and neomycin sulphate (red), which remained stable throughout the simulation, indicating a high level of compactness in the protein.

SASA AND H-BOND:

The SASA was measured to analyze the compactness of the hydrophobic core, where the changes in SASA over time for the Indirubin and Neomycin Sulphate protein complex was studied and shown in Fig. 6. The average SASA value from 0 to 100 ns for the Indirubin and Neomycin Sulphate protein complex proteins were 161.01+/-4.45 nm and 160.46+/-3.51 nm, respectively. The results suggest that there were no changes in the structural level of the proteins throughout the simulation. Figure 7displays the hydrogen bond analysis results for the complexes involving Indirubin and Neomycin Sulphate. The

plot clearly shows that both ligands possess a significant number of hydrogens indicating stable protein ligand complex.

MM-PBSA

MM-PBSA analysis revealed that indirubin has more stable and favorable binding affinity when compared to neomycin sulphate. Indirubins strong van der Waals interaction and lower energy fluctuations indicates its superior binding stability. Thus, indicates indirubin is more efficient ligand for target protein. Table 3 shows a comparison of their binding strength as inhibitors, calculated using the MM-PBSA method.

Table 3
Binding free energy calculation of Indirubin and Neomycin sulphate

System	Van der Waal energy	Electrostatic energy	Polar solvation energy	Binding energy
Indirubin	-148.937 +/- 5.789 kJ/mol	-32.248 +/- 5.754 kJ/mol	122.777 +/- 12.153 kJ/mol	-15.699 +/- 0.769 kJ/mol
Neomycin Sulphate	-44.975 +/- 20.212 kJ/mol	-24.216 +/- 91.152 kJ/mol	10.839 +/- 50.370 kJ/mol	-52.177 +/- 79.517 kJ/mol

ANTIBACTERIAL EFFICIENCY OF PLANT EXTRACTS

Antibacterial analysis of fresh and dry leaf extract of *Wrightia tinctoria* was evaluated against multi drug resistant *S. aureus*. Among all the tested extracts, the dry leaf ethyl acetate extract demonstrated the highest antibacterial activity, as evidenced by the largest zone of inhibition (ZI). Thus indicates that the active compounds responsible for antibacterial activity may be more concentrated or more stable in the dry form compared to the fresh extract or the other parts of the plant. In contrast, extracts from other parts of *W. tinctoria*, showed comparatively lower antibacterial effects, with smaller zones of inhibition.

The antibacterial activity of *W. tinctoria* was most pronounced in the dry leaf ethyl acetate, which, at a concentration of 100 µg, demonstrated the highest zone of inhibition measuring 26.33 ± 0.33 mm. This was followed by the fresh leaf ethyl acetate extract, which showed considerable activity with a zone of inhibition of 12.00 ± 0.57 mm. In contrast, extracts from the bark and seeds of *W. tinctoria* exhibited only low to moderate antibacterial activity. Graphical representations of the antibacterial activity of the dry and fresh leaf extracts of *W. tinctoria* were generated using GraphPad Prism 5 (Fig. 8 and Fig. 9)

ANTIBIOTIC SUSCEPTIBILITY ANALYSIS

The multi-drug resistance profile of *S. aureus* was assessed using the disc diffusion method, involving nine different antibiotics at various concentrations. The results were categorized as sensitive (S), intermediate resistant (I), and resistant (R) in accordance with the Clinical and Laboratory Standards

Institute (CLSI) guidelines. Among the antibiotics tested, *S. aureus* exhibited 100% resistance to methicillin, streptomycin, vancomycin, colistin, and piperacillin. Intermediate resistance was observed with azithromycin and imipenem. Notably, *S. aureus* showed significant susceptibility to neomycin sulphate, which produced the highest zone of inhibition, followed by tetracycline. The antibiogram results clearly indicate that approximately 70% of the antibiotics tested were ineffective against *S. aureus* (Fig. 10). This highlights the strain's extensive resistance and underscores the need for alternative treatment options or the development of new antibacterial agents.

Note

AZM denotes azithromycin, CL- colistin, IP – imipenem, NS- Neomycin Sulphate, MET- Methicillin, PI- Piperacillin, S- streptomycin, TE- Tetracycline, VA- vancomycin. The error bar, with a significance level of P 0.05, represent the standard error of the mean value.

GC-MS PROFILING

The GC-MS analysis of the EALE of *W. tinctoria* revealed the presence of 50 phytocompounds. Among these, the compound with the highest peak area was indirubin, an alkaloid, which constituted 6.59% of the total extract. Other significant compounds identified as 9,19-cyclolanost-24-en-3-ol, (3.beta.) with a peak area of 17.36%, β-sitosterol (11.11%), stigmast-5-en-3-ol, (3.beta.) (8.69%), norolean-12-ene (5.37%), phytol (4.45%), palmitic acid (2.72%), urs-12-en-3beta-ol (2.01%) and indigo (1.39%). The detailed identification of these compound along with their retention time and compound ID was provides (Table 4) as well as the chromatogram of *W. tinctoria* EALE, illustrating these peaks (Fig. 11). This analysis highlights the complex phytochemical composition of *W. tinctoria*, with several compounds of potential pharmacological interest.

Table 4
GC MS profiling of ethyl acetate leaf extract of *Wrightia tinctoria*

S. No	Compound Name	Compound ID	Retention Time	Peak Area %
1	Tricyclo[4.4.0.0(2,7)]dec-3-ene, 1,3-dimethyl-8-(1-methylethyl)	6432119	14.734	0.20
2	Bicyclo[7.2.0]undec-4-ene, 4,11,11-trimethyl-8-methylene	5281515	15.977	0.38
3	1,4,8-cycloundecatriene, 2,6,6,9-tetramethyl	5281520	16.943	0.25
4	Ethanone, 1-(2-methyl-1-cyclopenten-1-yl)	137847	21.095	0.16
5	Sulfurous acid, 2-ethylhexyl isohexyl ester	6420722	21.180	0.33
6	Acetic acid, 1,7,7-trimethyl-bicyclo[2.2.1]hept-2-yl ester	6448	21.332	0.46
7	Hexadecanal	984	23.411	0.32
8	Octahydro-1,8a(1h)-naphthalenediol	574054	24.795	0.71
9	Diethyl Phthalate	6781	26.524	1.91
10	3-Eicosyne	549159	27.000	0.22
11	2H-Pyran, 2-(2-heptadecynyloxy)tetrahydro	544115	27.073	0.29
12	3,7,11,15-Tetramethyl-2-hexadecen-1-ol	5366244	27.379	0.56
13	Palmitic acid	985	28.364	2.72
14	Phytol	5280435	31.602	4.45
15	9,12,15-Octadecatrienoic acid	5280934	31.884	0.89
16	Oleic Acid	445639	31.985	0.33
17	Oleanolic acid	10494	32.317	0.24
18	Octadecanoic acid	5281	32.445	0.33
19	2-biphenylethylamine, 5-methoxy-, hydrochloride	25946	33.443	0.49
20	24-Methylenecycloartanol	94204	35.108	0.31
21	Squalene	638072	36.739	0.28
22	Copaene	12303902	38.306	0.23
23	Tritriacontane	12411	39.819	0.16
24	Hexatriacontane	12412	41.279	0.20
25	Indirubin	638072	42.875	6.59

S. No	Compound Name	Compound ID	Retention Time	Peak Area %
26	Isatin	7054	44.368	0.87
27	2,6,10,14-Hexadecatetraen-1-ol, 3,7,11,15-tetramethyl	86591503	44.466	0.34
28	17beta-Hydroxyl-28-norolean-12-ene-3,16-dione	102067273	44.539	1.35
29	2,2-dimethyl-3-(3,7,16,20-tetramethyl-heneicosa-3,7,11,15,19-pentaenyl)-oxirane	5367592	44.696	0.37
30	Solanesol	5477212	46.030	0.19
31	Ergost-5-en-3-ol	18660356	46.336	0.88
32	2h-1-benzopyran-6-ol, 3,4-dihydro-2,7,8-trimethyl-2-(4,8,12-trimethyltridecyl)	14986	46.628	1.00
33	β-caryophyllene oxide	1742210	46.778	0.24
34	Ursolic acid	64945	47.270	0.88
35	2-propyldecane-1,3,8,10- tetrol	88829318	47.759	0.52
36	17-Pentatriacontene	5365022	48.270	0.35
37	2,5,7,8-tetramethyl-2-(4,8,12-trimethyltridecyl)-3,4-dihydro-2h-chromen-6-yl hexofuranoside	597057	48.537	0.43
38	Tetrapentacontane	521846	48.733	1.03
39	Undecane	14257	48.840	0.90
40	Urs-12-en-3beta-ol	73170	49.490	2.01
41	2,3,3-Trimethyl-2-(methyl pentanoyl)-cyclopentanone	573846	50.840	2.42
42	Indigo	10215	51.820	1.39
43	9,19-cyclolanostan-3-ol, 24-methylene-, (3.beta)	94204	52.434	1.28
44	Stigmast-5-en-3-ol, (3.beta)	222284	53.800	8.69
45	β- Tocopherol	6857447	54.195	1.02
46	6-Ethyl-2-methyldecane	43923	54.465	5.37
47	Neophytadiene	10446	54.882	12.66
48	β- Sitosterol	225688	55.977	11.11
49	9,19-Cyclolanost-24-en-3-ol, (3.beta)	92110	56.249	17.36
50	Lanosterol	246983	56.505	1.33

DISCUSSION

Staphylococcus aureus being a pervasive pathogen found in both hospital and community settings, poses significant public health risks. The misuse and overuse of antibiotics have exacerbated drug resistance issues in treating *S. aureus* infections (Ahmed et al., 2024). According to Mancuso *et al.*, (2021), diseases caused by multidrug-resistant bacteria result in approximately 700,000 deaths annually. The presence of multiple virulence mechanisms is particularly concerning due to limited treatment options. These mechanisms enable the bacteria to evade the host's immune response and include colonization of host tissues, leading to conditions such as bloodstream infections, skin infections, necrotizing pneumonia, and other severe tissue infections (Mlynarczyk-Bonikowska et al., 2022). Medicinal plants offer a rich source of bioactive compounds that, when combined, can potentially enhance therapeutic efficacy through synergistic effects against a wide range of multidrug-resistant pathogens (Huang et al., 2022). Ejaz et al. 2014 demonstrated that plant-based strategies work significantly in inhibiting multidrug resistant bacteria notable *S. aureus*. In a similar vein a research by Panda et al. 2020also confirmed this, both of them investigated the anti-staphylococcal activity of many traditional medicinal herbs from Pakistan and India. Thus, the study offers a broad perspective on the bactericidal characteristics of medicinal plants in combating against antibiotic resistance by focusing on various geographic regions and plant species. Similarly, our research focuses on evaluating the potential of phytocompounds from eight medicinal plants known for their remarkable biological properties. Researches have demonstrated that cell wall-anchored proteins are pivotal in facilitating bacterial infections by enabling attachment to specific host tissues. Clumping factor A, for instance, exemplifies such a protein by promoting bacterial adhesion to host tissue fibrinogen, thereby initiating infection (Foster 2019; Speziale and Pietrocola, 2020; Viljoen et al., 2021).In the current study, initially ADME profiling was conducted thereby explored the drug-likeness tests to mitigate the risk of late-stage drug failure rates specifically during clinical trials (Panigrahiet al., 2020). Where 19 compounds found to have drugs like properties meeting all necessary parameters and demonstrating favorable pharmacokinetic properties including absorption, distribution, and metabolic stability. Subsequently, Glide module of Schrodinger suite utilizes a grid-based approach to predict ligand binding sites within the target protein and employed an extra precision scoring function during the analysis (Sankar and Engels 2018). As a result,15bioactive compounds demonstrated robust binding interactions with the target protein, achieving an average Glide score ranging from − 8 to -2 kcal/mol. These compounds effectively interacted with specific amino acid residues such as ILE (isoleucine), GLY (glycine), ASN (asparagine), and GLU (glutamic acid), by forming hydrogen bonds with residues including ILE 339, 384, ASN 525, 286, GLU 526, and residue 342. The presence of these amino acid residues was confirmed through active site prediction tool. The phytocompounds with their least G scores were detailed in Table 8. Indirubin derived from *W. tinctoria* demonstrated the highest binding affinity with the target protein ClfA, forming hydrogen bonds with glycine and isoleucine residues. In a similar vein, following ADME profiling, Ragi *et al.* (2021) used AutoDock 4.20 to dock a variety of virulence proteins, including ClfA, with its sniff base chemical. Potent binding capacities with the target protein and interactions with the amino acid residues valine, lysine, isoleucine, and glycine are characteristics of their study that are consistent with our findings. In

another investigation by Wadapurkar et al. (2018), out of 86 plant-derived anti-staphylococcal compounds, 46 were deemed suitable for docking analysis. Among which the acetylated abietane quinone derived from mint leaves exhibited a good binding affinity with a G score of -7.52 kcal/mol, while in our study, the top-performing compound indirubin showed a maximum binding energy of -8.82 kcal/mol. Traditionally, Indirubin, extracted from *W. tinctoria*, were used for treating skin infections and has been documented for its potent antibacterial activity against both Gram-positive and Gram-negative bacteria. Reports also unfold their superior efficacy against *S. aureus* comparatively with standard antibiotics like ciprofloxacin and streptomycin (Kale et al., 2021; Ponnusamy et al., 2010). Additionally, Tanaka et al., (2019) studied the wound-healing properties of indirubin and found that it accelerates the healing process. Indigo, the second-best docked compound, exhibits diverse biological properties including anti-pyretic and anti-inflammatory activities (Xu*et al.*, 2021).Recently studies by yokote et al. (2023) suggests that compound indirubin and indigo are capable in treating ferroptosis, a cell death induced by oxidative stress, highlighting its role as a promising drug target for ulcerative colitis. The results of MD simulations showed that, indirubin-receptor complex was found to be stable over the duration of100 ns. The RMSD analysis of thereceptor-indirubin and the receptor -neomycin sulphate complexes shows that the two structures differed minimally in their conformations. The neomycin sulphate complex had a marginally higher RMSD value of 0.2 nm while the indirubin complex maintained a lower RMSD value of 0.18 nm meaning that it had better structural stability. Furthermore, there was minimal fluctuations of the amino acids residues within both the complexes as revealed by RMSF analysis. Hydrogen bonding interactions, which are one of the essential factors in assessing the stability of protein-ligand complexes (Joshi et al., 2022) were investigated in detail. Both the docked complexes displayed several stable hydrogen bonds, as demonstrated in Fig. 7, indicating strong binding interactions. Table 5 consolidated free energy computations that induced the effects of polar solvation, electrostatics, Van der Waals forces, and binding energy. In comparison, Tiwari et al. (2022) Performed docking and dynamics simulations for compounds isolated from *Sisymbriumirio*, suggesting that a 70 ns simulation resulted in minimal structural deviation without loss of receptor-ligand complex stability. In line with this, our study based on these simulations demonstrates that indirubin does have the ability to stabilize the compactness and structural integrity of the receptor. By targeting ClfA, phytocompounds from the plant *W. tinctoria* were shown to have improved staphylococcal activity, according to these in silico investigations. We performed an invitro antibacterial investigation of this plant and then GC-MS phytochemical profiling to confirm these findings.

According to preliminary antibacterial screening results, the ethyl acetate extract of dried *W. tinctoria* leaves exhibited a more significant growth inhibition against *S. aureus* than other extracts These results are in accordance with previous studies from Srivastava (2014), who revealed that methanolic extracts of *W. tinctoria* bark and leaves showed potent inhibition activity against *S. aureus*. In fact, the leaf extracts exhibited more significant antimicrobial potential than bark and seed extracts. This would likely be due to differences in the phytochemical composition driven by geographical loci, environmental conditions, and extraction methods among others (Liuet al., 2018). In addition to the antibacterial screening, antibiotic susceptibility testing was conducted on *S. aureus*. The findings revealed that the

bacterium exhibited resistance to 70% of the antibiotics tested. This aligns with a study by (Akanbiet al., 2017), which reported that *S. aureus* isolated from beef samples showed resistance to 83% of antibiotics tested, including amoxicillin, chloramphenicol, ciprofloxacin, ceftriaxone, gentamicin, and trimethoprim. Moreover, demonstrated intermediate resistance to tetracycline and azithromycin. Similarly, in our study, azithromycin and imipenem showed intermediate resistance, with zones of inhibition measuring 10 mm and 8 mm, respectively. The small zones of inhibition observed suggest a heightened risk of developing antibiotic resistance. Following GC-MS profiling, the ethyl acetate extract of the dried leaves of *W. tinctoria* revealed a wide range of bioactive compounds, including ursolic acid, diethyl phthalate, lupeol, stigmasterol, lupeol, squalene, isatin, β-sitosterol, indirubin, and 41 others. Different phytochemical compositions of *W. tinctoria* extracts have been reported in other similar research. Sheela et al. (2021) reported 12 compounds from ethyl acetate extracts, whereas Khan et al. (2021) reported 28 compounds, including phytol, stigmast-5-en-3-ol, and β-caryophyllene. These variations rely on the plant's maturity, harvesting conditions, and extraction method (Liu et al., 2018). Even while the antibacterial properties of different sections of *W. tinctoria* have been studied in great detail, nothing is known about the precise mechanisms by which these effects are achieved. Using in silico methods could successfully solve this knowledge gap. Therefore, our study's findings indicate that *W. tinctoria* that contains indirubin has a lot of potential as an anti-staphylococcal agent.

CONCLUSION

The current studyunderline the therapeutic promise of *W. tinctoria* and its bioactive constituents in combating bacterial infections, including those due to drug-resistant strains. Highlighting In silico approaches by bridging the gap and provide useful insight into the molecular interactions of its bioactive compounds. Our combined in silico and in vitro studies highlight that bioactive compounds specificcally *W. tinctoria* extracts is capable of being a promising anti-staphylococcal agent with stability in binding to the receptors, and also it is highly active as an antibacterial. Further therapeutic studies have to be conducted on indirubin, as well as other bioactive molecules in *W. tinctoria*, against the particular *Staphylococcus aureus* and drug-resistant bacterial strains. Thus, the results from our studies strongly suggest that indirubin holds considerable promise as an anti-staphylococcal agent.

Abbreviations

ClfA- Clumping factor A, WHO- World Health Organization, ADME- Absorption, Distribution, Metabolism, and Excretion, PDB- Protein Data Bank, RMSD-Root Mean Square Deviation, RMSF- Root Mean Square Fluctuation, RG-Radius of Gyration, SASA- Solvent accessible surface area, H-Bond- Hydrogen Bond, MM-PBSA- Molecular Mechanics Poisson-Boltzmann surface area, LIG-Ligand.

Declarations

ACKNOWLEDGEMENT

The authors are grateful to the Kongunadu Arts and Science College administration for supplying all software required to complete this project.

FUNDING

No funding was received for conducting this study.

ETHICAL APPROVAL

This article does not contain any studies involving animals and human participants by any of the authors.

DISCLOSURE STATEMENT

The authors declared that they have no conflict of interest in the studies.

DATA AVAILABILITY STATEMENT.

The authors confirm that the Data used and/or analyzed in the present study are available within the article.

AUTHOR CONTRIBUTION

Vidya S. L: Carried out the studies, Data curation, and Drafted the manuscript and software. Anantha Bhairavi V: Formal analysis and Validation. R. Sathishkumar: Designed the study and Supervision.

The final manuscript was read and approved by all authors.

References

1. Ahmed, S. K., Hussein, S., Qurbani, K., Ibrahim, R. H., Fareeq, A., Mahmood, K. A., & Mohamed, M. G. (2024). Antimicrobial resistance: Impacts, challenges, and future prospects. Journal of Medicine, Surgery, and Public Health, 2, 100081. https://doi.org/10.1016/j.glmedi.2024.100081
2. Akanbi, O. E., Njom, H. A., Fri, J., Otigbu, A. C., & Clarke, A. M. (2017). Antimicrobial Susceptibility of Staphylococcus aureus Isolated from Recreational Waters and Beach Sand in Eastern Cape Province of South Africa. International Journal of Environmental Research and Public Health, 14(9), 1001. https://doi.org/10.3390/ijerph14091001
3. Babar, M. M., Zaidi, N.-S. S., Pothineni, V. R., Ali, Z., Faisal, S., Hakeem, K. R., & Gul, A. (2017). Application of Bioinformatics and System Biology in Medicinal Plant Studies. Plant Bioinformatics, 375–393. https://doi.org/10.1007/978-3-319-67156-7_15
4. Bauer, A. W., Kirby, W. M. M., Sherris, J. C., &Turck, M. (1966). Antibiotic Susceptibility Testing by a Standardized Single Disk Method. American Journal of Clinical Pathology, 45(4_ts), 493–496. https://doi.org/10.1093/ajcp/45.4_ts.493

5. Bhairavi, V. A., Vidya, S. L., & Sathishkumar, R. (2023). Identification of effective plant extracts against candidiasis: an in silico and in vitro approach. Future Journal of Pharmaceutical Sciences, 9(1). https://doi.org/10.1186/s43094-023-00489-x
6. Bhatia, P., Sharma, A., George, A. J., Anvitha, D., Kumar, P., Dwivedi, V. P., & Chandra, N. S. (2021). Antibacterial activity of medicinal plants against ESKAPE: An update. Heliyon, 7(2), e06310. https://doi.org/10.1016/j.heliyon.2021.e06310
7. Bhattacharya, M., &Horswill, A. R. (2024). The role of human extracellular matrix proteins in defining Staphylococcus aureus biofilm infections. FEMS Microbiology Reviews, 48(1). https://doi.org/10.1093/femsre/fuae002
8. Cardoza, S., Singh, A., Sur, S., Singh, M., Dubey, K. D., Samanta, S. K., Mandal, A., & Tandon, V. (2024). Computational investigation of novel synthetic analogs of C-1'β substituted remdesivir against RNA-dependent RNA-polymerase of SARS-CoV-2. Heliyon, 10(17), e36786. https://doi.org/10.1016/j.heliyon.2024.e36786
9. Ejaz, R., Ashfaq, U. A., & Idrees, S. (2014). Antimicrobial potential of Pakistani medicinal plants against multi-drug resistance Staphylococcus aureus. *J Coast Life Med*, *2*(9), 714-20.https://doi.org/10.12980/jclm.2.201414b1
10. Filimonov, D. A., Lagunin, A. A., Gloriozova, T. A., Rudik, A. V., Druzhilovskii, D. S., Pogodin, P. V., &Poroikov, V. V. (2014). Prediction of the Biological Activity Spectra of Organic Compounds Using the Pass Online Web Resource. Chemistry of Heterocyclic Compounds, 50(3), 444–457. https://doi.org/10.1007/s10593-014-1496-1
11. Foster, T. J. (2019). The MSCRAMM Family of Cell-Wall-Anchored Surface Proteins of Gram-Positive Cocci. Trends in Microbiology, 27(11), 927–941. https://doi.org/10.1016/j.tim.2019.06.007
12. Gangadharappa, B. S., Rajashekarappa, S., & Sathe, G. (2020). Proteomic profiling of Serratia marcescens by high-resolution mass spectrometry. BioImpacts, 10(2), 123–135. https://doi.org/10.34172/bi.2020.15
13. Hasan, R., Acharjee, M., & Noor, R. (2016). Prevalence of vancomycin resistant Staphylococcus aureus (VRSA) in methicillin resistant S. aureus (MRSA) strains isolated from burn wound infections. Tzu Chi Medical Journal, 28(2), 49–53. https://doi.org/10.1016/j.tcmj.2016.03.002
14. He, W., Liu, H., Wang, Z., Tay, F. R., & Shen, Y. (2024). The dynamics of bacterial proliferation, viability, and extracellular polymeric substances in oral biofilm development. Journal of Dentistry, 143, 104882. https://doi.org/10.1016/j.jdent.2024.104882
15. Herman-Bausier, P., Labate, C., Towell, A. M., Derclaye, S., Geoghegan, J. A., &Dufrêne, Y. F. (2018). clumping factor A is a force-sensitive molecular switch that activates bacterial adhesion. Proceedings of the National Academy of Sciences of the United States of America, 115(21), 5564–5569. https://doi.org/10.1073/pnas.1718104115
16. Higgins, J., Loughman, A., van Kessel, K. P. M., van Strijp, J. A. G., & Foster, T. J. (2006). Clumping factor A ofStaphylococcusaureusinhibits phagocytosis by human polymorphonuclear leucocytes. FEMS Microbiology Letters, 258(2), 290–296. https://doi.org/10.1111/j.1574-6968.2006.00229.x

17. Huang, W., Wang, Y., Tian, W., Cui, X., Tu, P., Li, J., Shi, S., & Liu, X. (2022). Biosynthesis Investigations of Terpenoid, Alkaloid, and Flavonoid Antimicrobial Agents Derived from Medicinal Plants. Antibiotics, 11(10), 1380. https://doi.org/10.3390/antibiotics11101380
18. Jegadeeshwari, A., Seelam, N. R., & Myneni, V. R. (2023). Evaluation of Antibacterial and Anticancer Characteristics of Silver Nanoparticles Synthesized from Plant Extracts of Wrightia tinctoria and Acacia chundra. International Journal of Analytical Chemistry, 2023, 1–14. https://doi.org/10.1155/2023/6352503
19. Joshi, C., Chaudhari, A., Joshi, C., Joshi, M., &Bagatharia, S. (2022). Repurposing of the herbal formulations: molecular docking and molecular dynamics simulation studies to validate the efficacy of phytocompounds against SARS-CoV-2 proteins. *Journal of biomolecular structure & dynamics*, *40*(18), 8405–8419. https://doi.org/10.1080/07391102.2021.1922095
20. K, R., Kakkassery, J. T., Raphael, V. P., Johnson, R., & K, V. T. (2021). In vitro antibacterial and in silico docking studies of two Schiff bases on Staphylococcus aureus and its target proteins. Future Journal of Pharmaceutical Sciences, 7(1). https://doi.org/10.1186/s43094-021-00225-3
21. Kale, N., Rathod, S., More, S., & Shinde, N. (2021). Phyto-Pharmacological Profile of Wrightia tinctoria. Asian Journal of Research in Pharmaceutical Sciences, 301–308. Internet Archive. https://doi.org/10.52711/2231-5659.2021.00047
22. Khan, N., Ali, A., Qadir, A., Ali, A., Warsi, M. H., Tahir, A., & Ali, A. (2021). GC-MS Analysis and Antioxidant Activity ofWrightia tinctoriaR.Br. Leaf Extract. Journal of AOAC INTERNATIONAL, 104(5), 1415–1419. https://doi.org/10.1093/jaoacint/qsab054
23. Liu, Y., Chen, P., Zhou, M., Wang, T., Fang, S., Shang, X., & Fu, X. (2018). Geographic Variation in the Chemical Composition and Antioxidant Properties of Phenolic Compounds from Cyclocaryapaliurus (Batal) Iljinskaja Leaves. Molecules, 23(10), 2440. https://doi.org/10.3390/molecules23102440
24. Mancuso, G., Midiri, A., Gerace, E., & Biondo, C. (2021). Bacterial Antibiotic Resistance: The Most Critical Pathogens. Pathogens, 10(10), 1310. https://doi.org/10.3390/pathogens10101310
25. Mishra, G. P., Bhadane, R. N., Panigrahi, D., Amawi, H. A., Asbhy, C. R., & Tiwari, A. K. (2021). The interaction of the bioflavonoids with five SARS-CoV-2 proteins targets: An in silico study. Computers in Biology and Medicine, 134, 104464. https://doi.org/10.1016/j.compbiomed.2021.104464
26. Mitra, D., Mitra, D., Sabri Bensaad, M., Sinha, S., Pant, K., Pant, M., Priyadarshini, A., Singh, P., Dassamiour, S., Hambaba, L., Panneerselvam, P., & Das Mohapatra, P. K. (2022). Evolution of bioinformatics and its impact on modern bio-science in the twenty-first century: Special attention to pharmacology, plant science and drug discovery. Computational Toxicology, 24, 100248. https://doi.org/10.1016/j.comtox.2022.100248
27. Mlynarczyk-Bonikowska, B., Kowalewski, C., Krolak-Ulinska, A., &Marusza, W. (2022). Molecular Mechanisms of Drug Resistance in Staphylococcus aureus. International Journal of Molecular Sciences, 23(15), 8088. https://doi.org/10.3390/ijms23158088
28. Moulishankar, A., &Sundarrajan, T. (2024). Pharmacophore, QSAR, molecular docking, molecular dynamics and ADMET study of trisubstituted benzimidazole derivatives as potent anti-tubercular

agents. Chemical Physics Impact, 8, 100512. https://doi.org/10.1016/j.chphi.2024.100512

29. Panda, S. K., Das, R., Lavigne, R., &Luyten, W. (2020). Indian medicinal plant extracts to control multidrug-resistant S. aureus, including in biofilms. South African Journal of Botany, 128, 283–291. https://doi.org/10.1016/j.sajb.2019.11.019
30. Panigrahi, D., Mishra, A., &Sahu, S. K. (2020). Pharmacophore modelling, QSAR study, molecular docking and insilico ADME prediction of 1,2,3-triazole and pyrazolopyridones as DprE1 inhibitor antitubercular agents. SN Applied Sciences, 2(5). https://doi.org/10.1007/s42452-020-2638-y
31. Patel, D. K., Patel, K., Duraiswamy, B., &Dhanabal, S. P. (2012). Phytochemical analysis and standardization of Strychnosnux-vomica extract through HPTLC techniques. Asian Pacific Journal of Tropical Disease, 2, S56–S60. https://doi.org/10.1016/s2222-1808(12)60124-8
32. Patidar, K., Panwar, U., Vuree, S., Sweta, J., Sandhu, M. K., Nayarisseri, A., & Singh, S. K. (2019). An In silico Approach to Identify High Affinity Small Molecule Targeting m-TOR Inhibitors for the Clinical Treatment of Breast Cancer. Asian Pacific Journal of Cancer Prevention, 20(4), 1229–1241. https://doi.org/10.31557/apjcp.2019.20.4.1229
33. Ponnusamy, K., Ramasamy, M., Savarimuthu, I., & Gabriel Paulraj, M. (2010). Indirubin potentiates ciprofloxacin activity in the NorA efflux pump of *Staphylococcus aureus*. Scandinavian Journal of Infectious Diseases. https://doi.org/10.3109/00365541003713630
34. Prasanth, D. S. N. B. K., Murahari, M., Chandramohan, V., Panda, S. P., Atmakuri, L. R., &Guntupalli, C. (2021). identification of potential inhibitors from against main protease and spike glycoprotein of SARS CoV-2. Journal of Biomolecular Structure & Dynamics, 39(13), 4618–4632.
35. Prlić, A., Kalro, T., Bhattacharya, R., Christie, C., Burley, S. K., & Rose, P. W. (2016). Integrating genomic information with protein sequence and 3D atomic level structure at the RCSB protein data bank. Bioinformatics, 32(24), 3833–3835. https://doi.org/10.1093/bioinformatics/btw547
36. Roy, S., Santra, S., Das, A., Dixith, S., Sinha, M., Ghatak, S., Ghosh, N., Banerjee, P., Khanna, S., Mathew-Steiner, S., Ghatak, P. D., Blackstone, B. N., Powell, H. M., Bergdall, V. K., Wozniak, D. J., & Sen, C. K. (2019). Staphylococcus aureus Biofilm Infection Compromises Wound Healing by Causing Deficiencies in Granulation Tissue Collagen. Annals of Surgery, 271(6), 1174–1185. https://doi.org/10.1097/sla.0000000000003053
37. Sahayarayan, J. J., Rajan, K. S., Vidhyavathi, R., Nachiappan, M., Prabhu, D., Alfarraj, S., Arokiyaraj, S., & Daniel, A. N. (2021). In-silico protein-ligand docking studies against the estrogen protein of breast cancer using pharmacophore based virtual screening approaches. Saudi Journal of Biological Sciences, 28(1), 400–407. https://doi.org/10.1016/j.sjbs.2020.10.023
38. Sankar, V., & Maida Engels, S. E. (2018). Synthesis, biological evaluation, molecular docking and in silico ADME studies of phenacyl esters of N-Phthaloyl amino acids as pancreatic lipase inhibitors. Future Journal of Pharmaceutical Sciences, 4(2), 276–283. https://doi.org/10.1016/j.fjps.2018.10.004
39. Sasikumar, A. P., Ramaswamy, S., & Sudhir, S. (2021). A scientific pharmacognosy on Gaucher's disease: an in silico analysis. Environmental Science and Pollution Research, 29(17), 25308–25317.

https://doi.org/10.1007/s11356-021-17534-y

40. Sheela, D., Abdul Rahim, M., Arunagirinadhan, N., Ramya, B., & Indra, V. (2021). GC-MS profiling and antibacterial activity of Wrightia tinctoria and Lantana camara leaves extract. *Intern. J. Zool. Invest*, *7*(2), 920-938. https://doi.org/10.33745/ijzi.2021.v07i02.084
41. Speziale, P., &Pietrocola, G. (2020). The Multivalent Role of Fibronectin-Binding Proteins A and B (FnBPA and FnBPB) of Staphylococcus aureus in Host Infections. Frontiers in Microbiology, 11. https://doi.org/10.3389/fmicb.2020.02054
42. Srivastava, R. (2014). A review on phytochemical, pharmacological, and pharmacognostical profile of Wrightia tinctoria: Adulterant of kurchi. Pharmacognosy Reviews, 8(15), 36. https://doi.org/10.4103/0973-7847.125528
43. Szymański, P., Markowicz, M., &Mikiciuk-Olasik, E. (2011). Adaptation of High-Throughput Screening in Drug Discovery—Toxicological Screening Tests. International Journal of Molecular Sciences, 13(1), 427–452. https://doi.org/10.3390/ijms13010427
44. Tanaka, Y., Uchi, H., Ito, T., &Furue, M. (2019). Indirubin-pregnane X receptor-JNK axis accelerates skin wound healing. Scientific Reports, 9(1). https://doi.org/10.1038/s41598-019-54754-2
45. Terreni, M., Taccani, M., &Pregnolato, M. (2021). New Antibiotics for Multidrug-Resistant Bacterial Strains: Latest Research Developments and Future Perspectives. Molecules, 26(9), 2671. https://doi.org/10.3390/molecules26092671
46. Thakur, M., Singh, K., &Khedkar, R. (2020). Phytochemicals. Functional and Preservative Properties of Phytochemicals, 341–361. https://doi.org/10.1016/b978-0-12-818593-3.00011-7
47. Tillotson, G. S., &Zinner, S. H. (2017). Burden of antimicrobial resistance in an era of decreasing susceptibility. Expert Review of Anti-Infective Therapy, 15(7), 663–676. https://doi.org/10.1080/14787210.2017.1337508
48. Tiwari, M., Gupta, S., & Bhargava, P. (2022). Virtual screening and molecular dynamics simulation studies to predict the binding of Sisymbriumirio L. derived phytochemicals against Staphylococcus aureus dihydrofolate reductase (DHFR). Journal of Applied and Natural Science, 14(4), 1297–1307. https://doi.org/10.31018/jans.v14i4.3641.
49. Viljoen, A., Viela, F., Mathelié-Guinlet, M., Missiakas, D., Pietrocola, G., Speziale, P., &Dufrêne, Y. F. (2021). Staphylococcus aureus vWF-binding protein triggers a strong interaction between clumping factor A and host vWF. Communications Biology, 4(1). https://doi.org/10.1038/s42003-021-01986-6
50. Wadapurkar, R. M., Shilpa, M. D., Katti, A. K. S., &Sulochana, M. B. (2018). In silico drug design for Staphylococcus aureus and development of host-pathogen interaction network. Informatics in Medicine Unlocked, 10, 58–70. https://doi.org/10.1016/j.imu.2017.11.002
51. Wang, E., Sun, H., Wang, J., Wang, Z., Liu, H., Zhang, J. Z. H., & Hou, T. (2019). End-Point Binding Free Energy Calculation with MM/PBSA and MM/GBSA: Strategies and Applications in Drug Design. Chemical Reviews, 119(16), 9478–9508. https://doi.org/10.1021/acs.chemrev.9b00055
52. Xu, xiaorong, Huang, S., Luo, C., Xu, R., Wang, F., He, Y., Yang, M., Lin, J., Han, L., & Zhang, D. (2023). Study on the antipyretic activity and potential mechanism of Indigo Naturalis on lipopolysaccharide-

induced fever rat model. https://doi.org/10.21203/rs.3.rs-3174972/v1

53. Yokote, A., Imazu, N., Umeno, J., Kawasaki, K., Fujioka, S., Fuyuno, Y., Matsuno, Y., Moriyama, T., Miyawaki, K., Akashi, K., Kitazono, T., &Torisu, T. (2023). Ferroptosis in the colon epithelial cells as a therapeutic target for ulcerative colitis. Journal of Gastroenterology, 58(9), 868–882. https://doi.org/10.1007/s00535-023-02016-4
54. Yuan, H., Ma, Q., Ye, L., & Piao, G. (2016). The Traditional Medicine and Modern Medicine from Natural Products. Molecules, 21(5), 559. https://doi.org/10.3390/molecules21050559
55. Yusof, I., &Segall, M. D. (2013). Considering the impact drug-like properties have on the chance of success. Drug Discovery Today, 18(13–14), 659–666. https://doi.org/10.1016/j.drudis.2013.02.008

Website Links

https://www.who.int/publications/i/item/9789240093461

https://www.who.int/publications/i/item/9789240093461

https://www.rcsb.org/

https://pubchem.ncbi.nlm.nih.gov/

http://www.way2drug.com/passonline/predict.php

Table 1

Tables 1 is available in the Supplementary Files section.

Figures

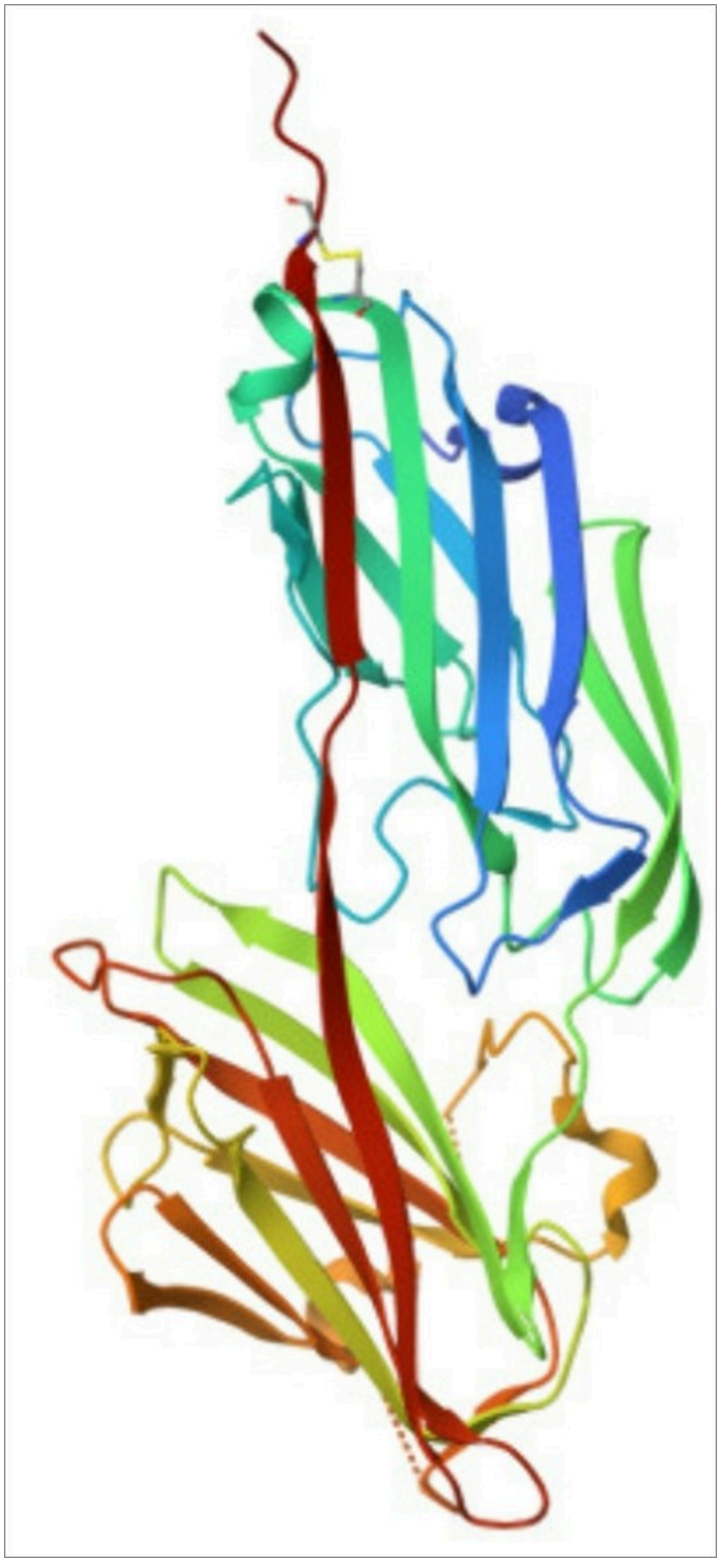

Figure 1

3D structure of the protein clumping factor A (ClFA) from *Staphylococcus aureus* (PDB ID: 2VR3)

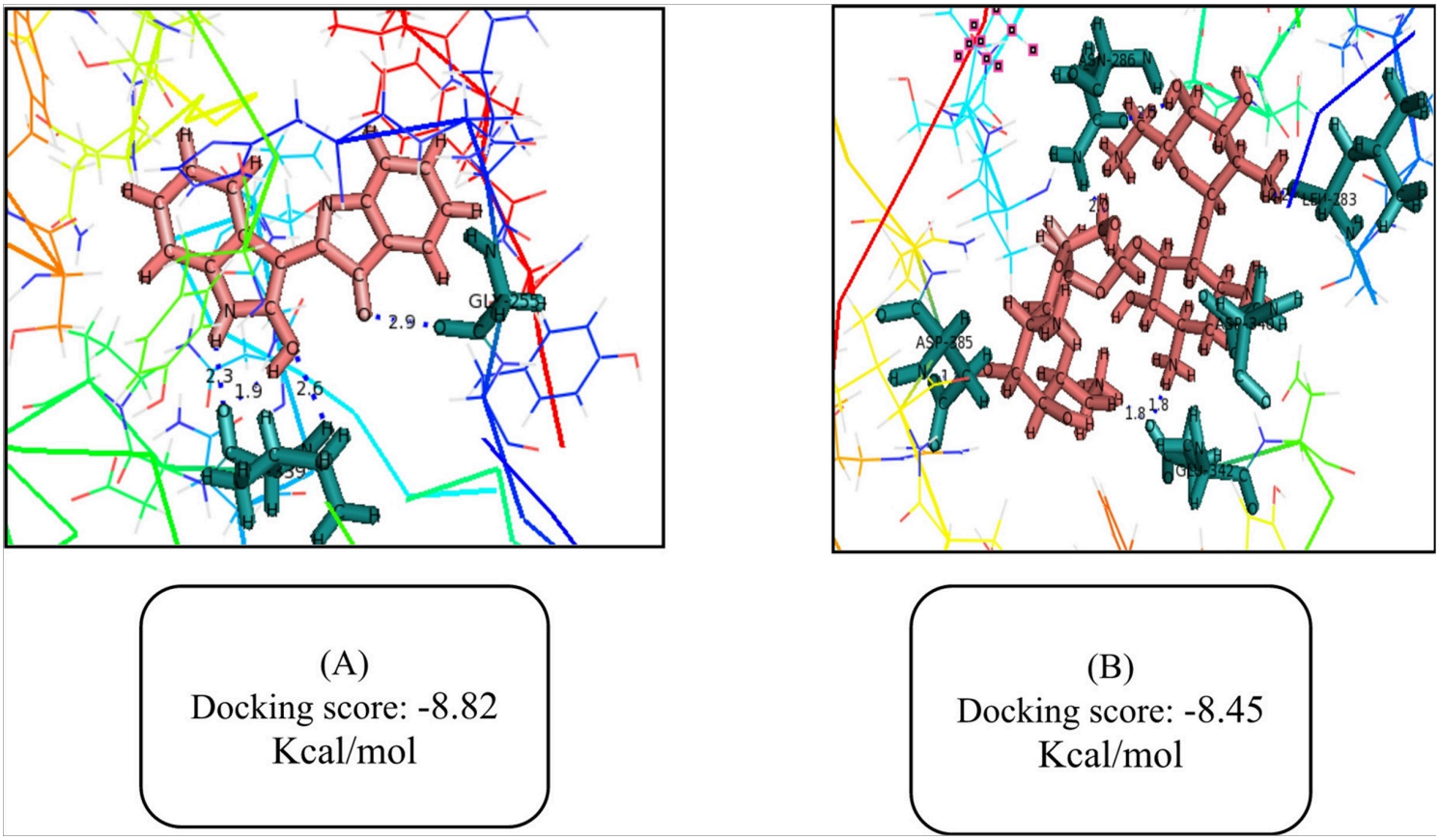

Figure 2

Figure 1. Hydrogen bond interaction with target protein Clumping factor A (ClfA: PDB-ID- 2VR3)

Note: The compounds are listed based on their G.score value (A) Indirubin; (B) Neomycin sulphate; the figure represents the hydrogen bond interaction of compound with the target protein along with Protein-ligand complex in space filling representation

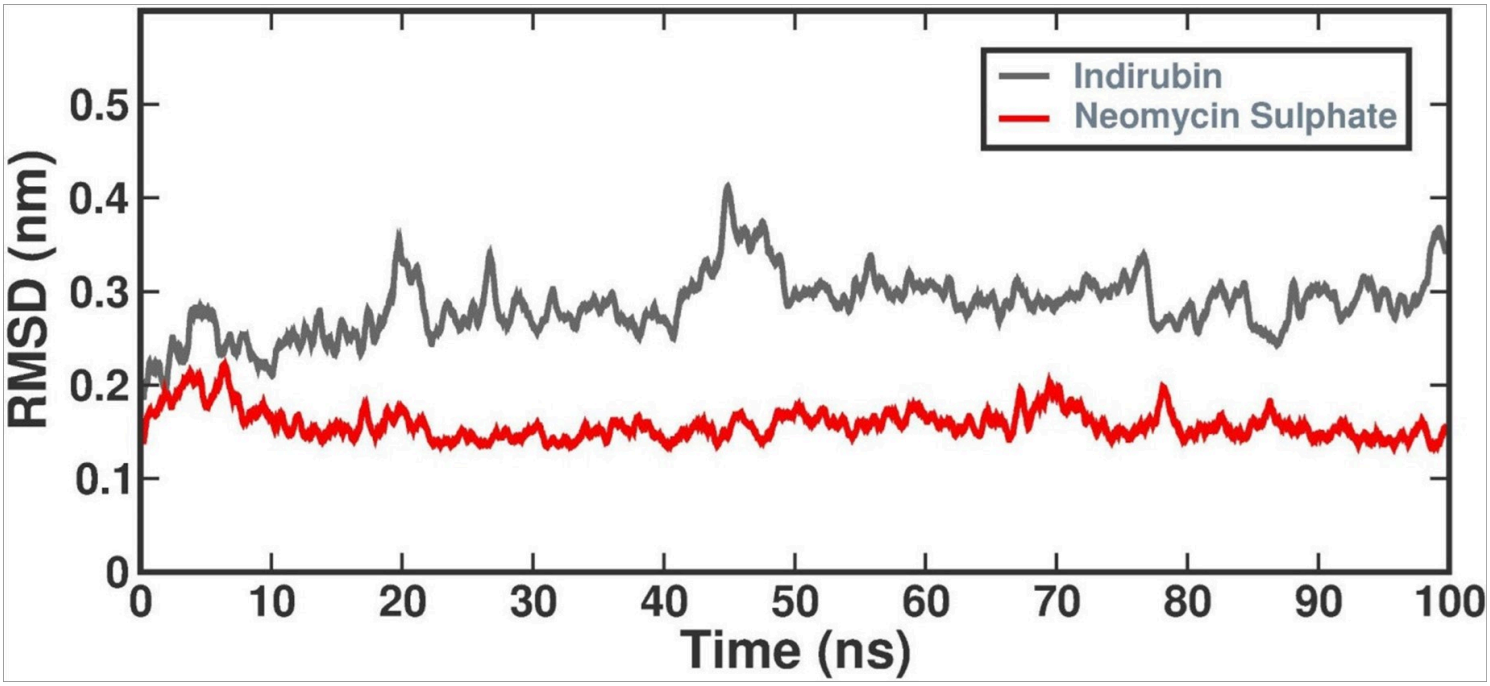

Figure 3

Figure 2. Root means square deviation of backbone atoms of Indirubin and Neomycin Sulphate

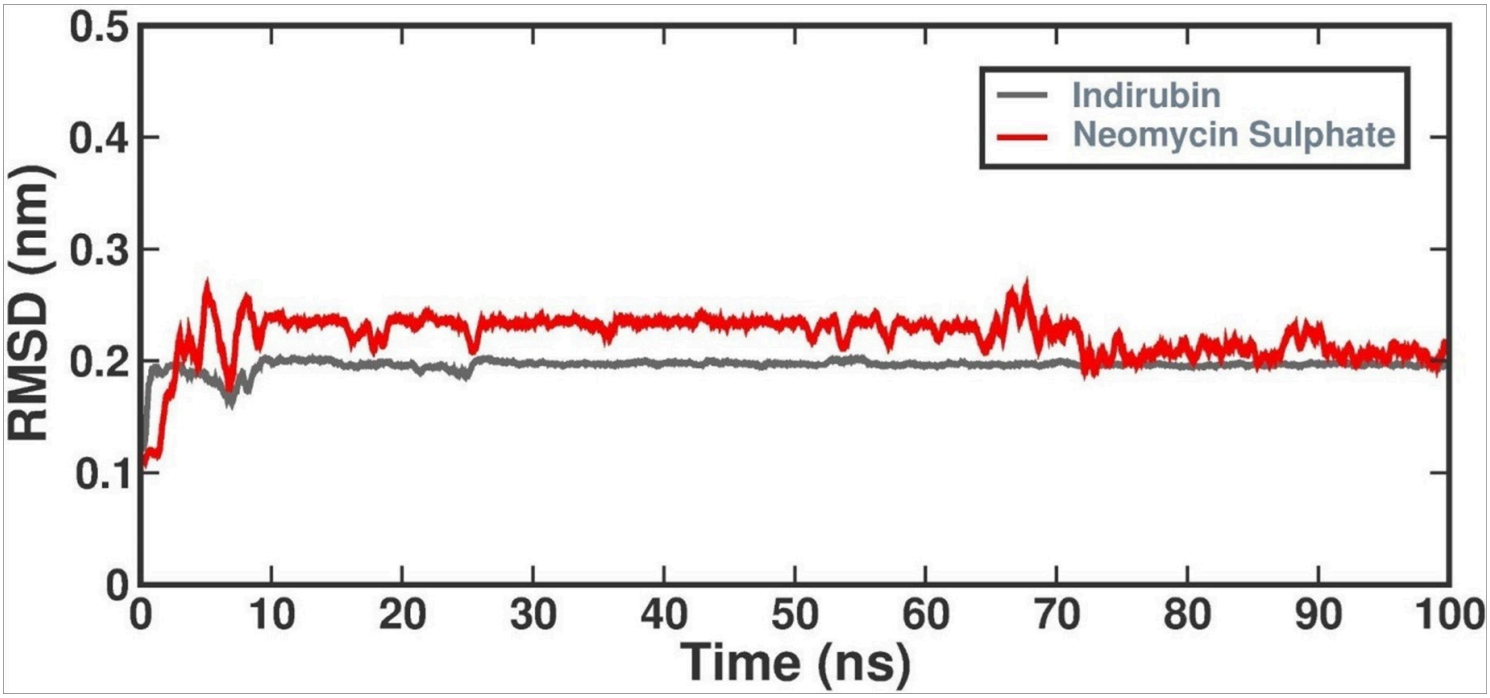

Figure 4

Figure 3. Ligand-Root means square deviation of backbone atoms of Indirubin and Neomycin Sulphate.

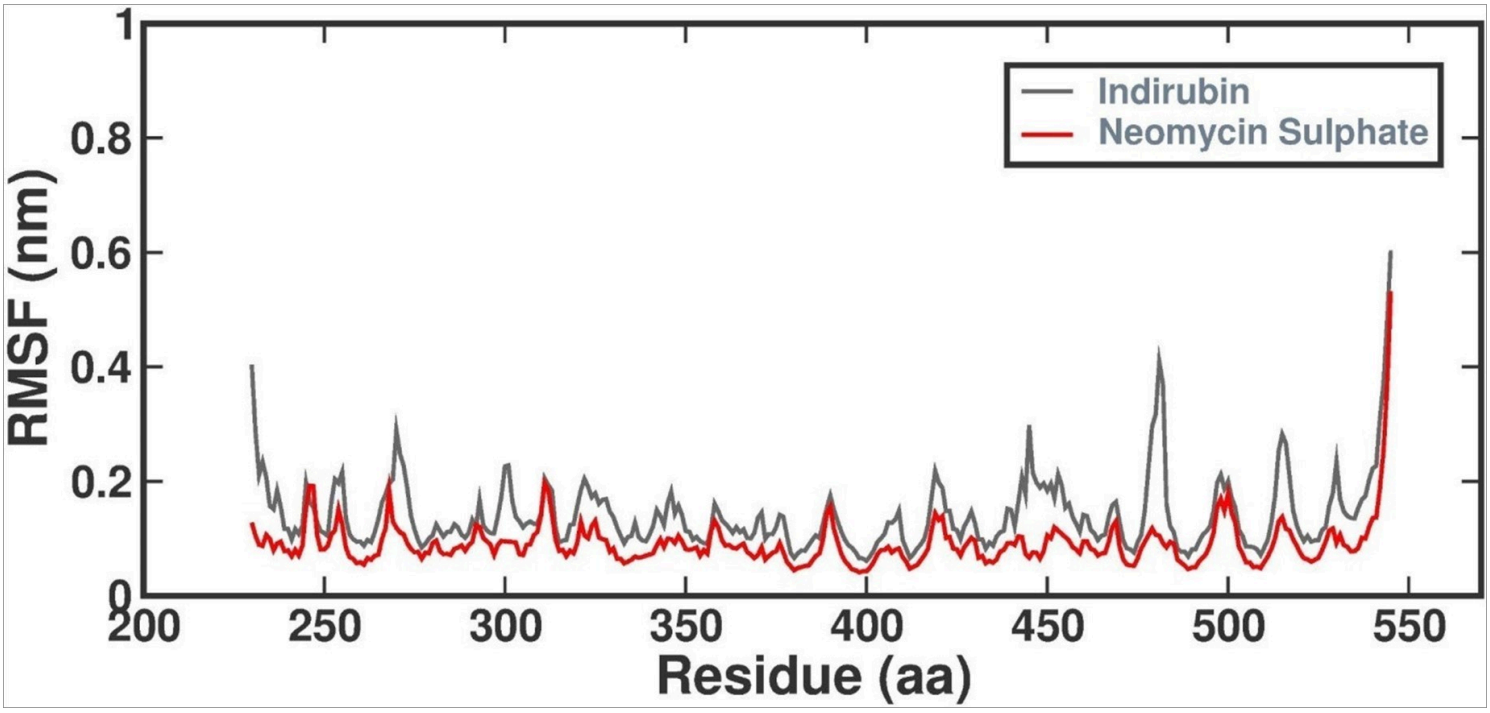

Figure 5

Figure 4. Root means square fluctuation of c-alpha atoms of Indirubin and Neomycin Sulphate

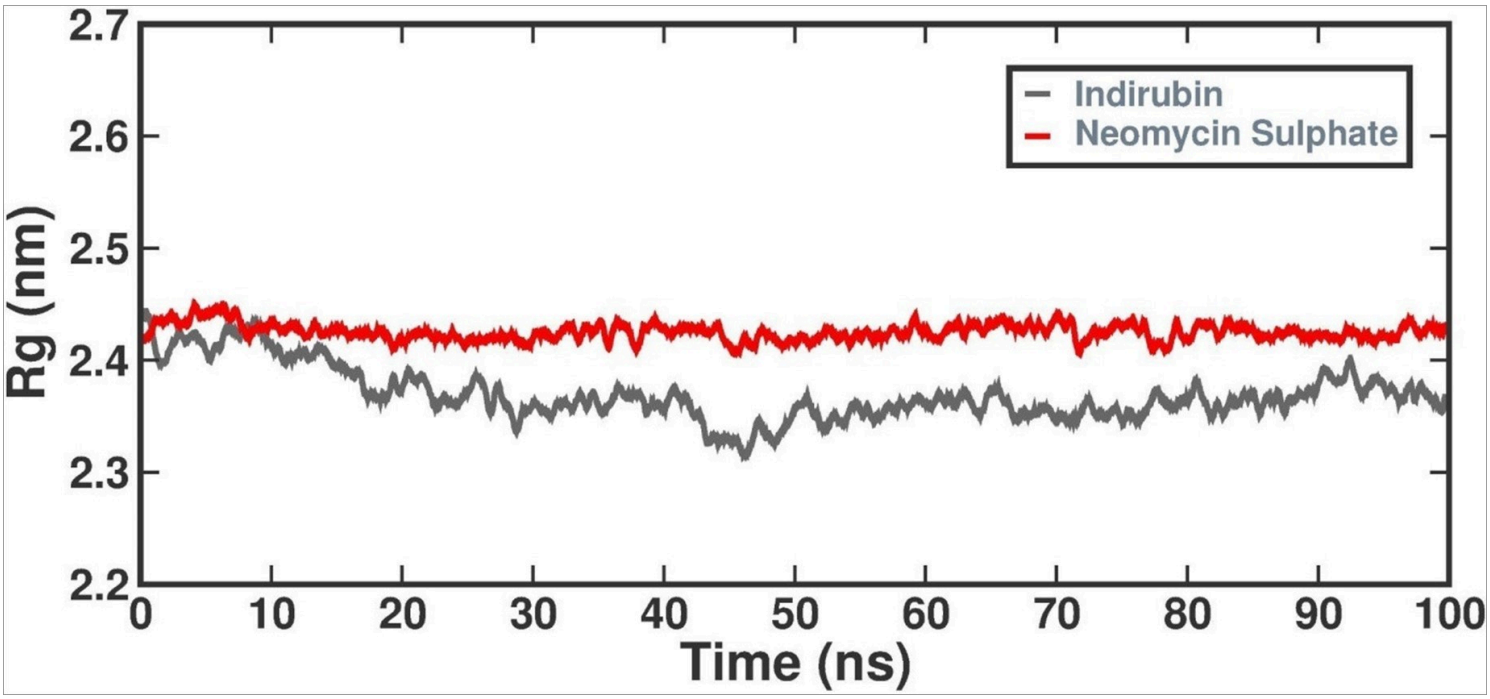

Figure 6

Figure 5. RG of backbone atoms with Indirubin and Neomycin Sulphate

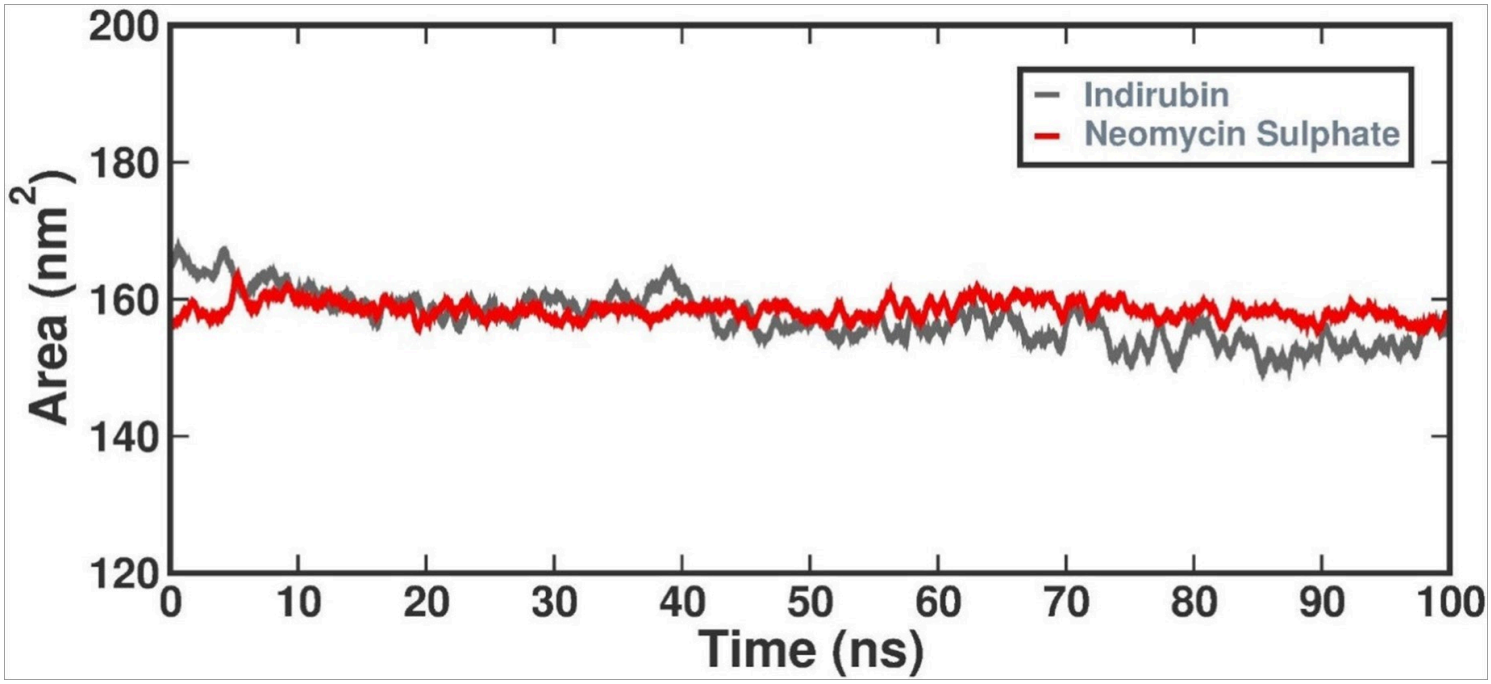

Figure 7

Figure 6. SASA of backbone atoms with Indirubin and Neomycin Sulphate

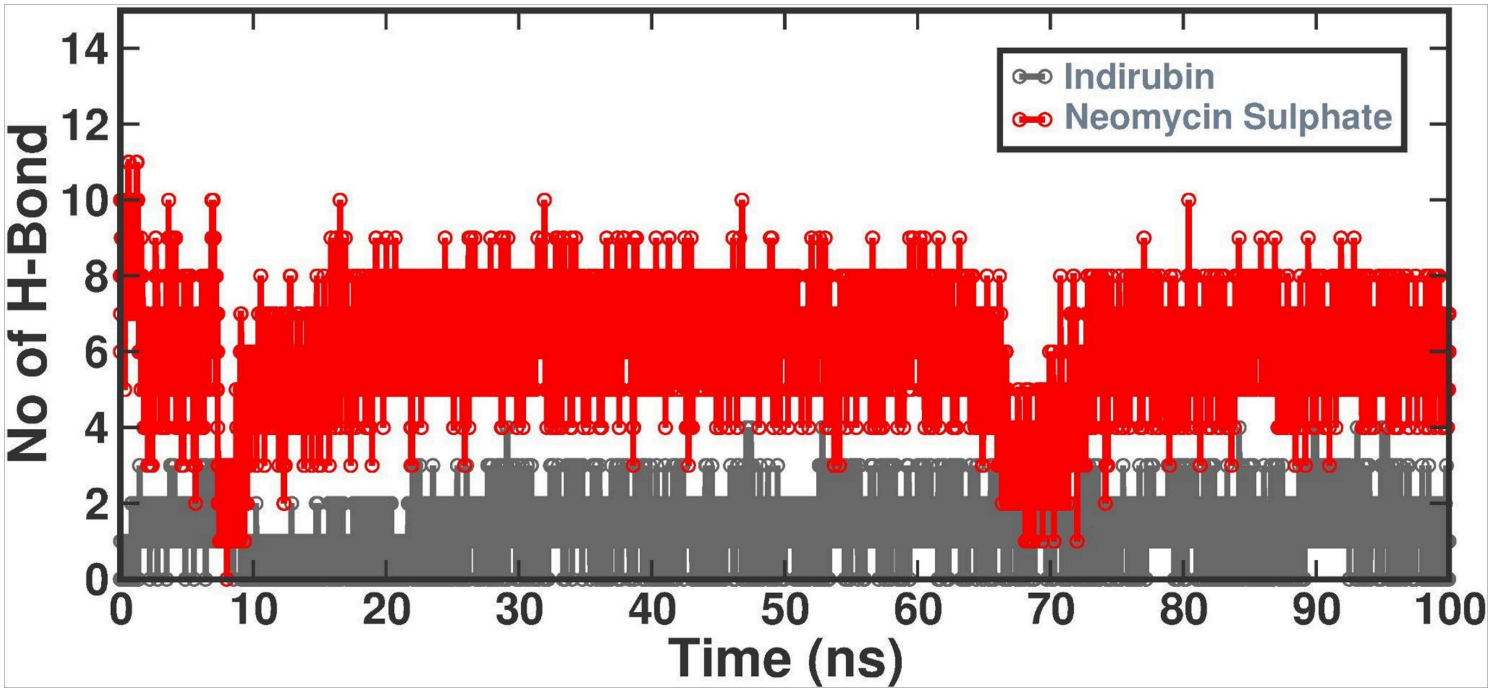

Figure 8

Fig. 7: H-Bond of Indirubin and Neomycin Sulphate

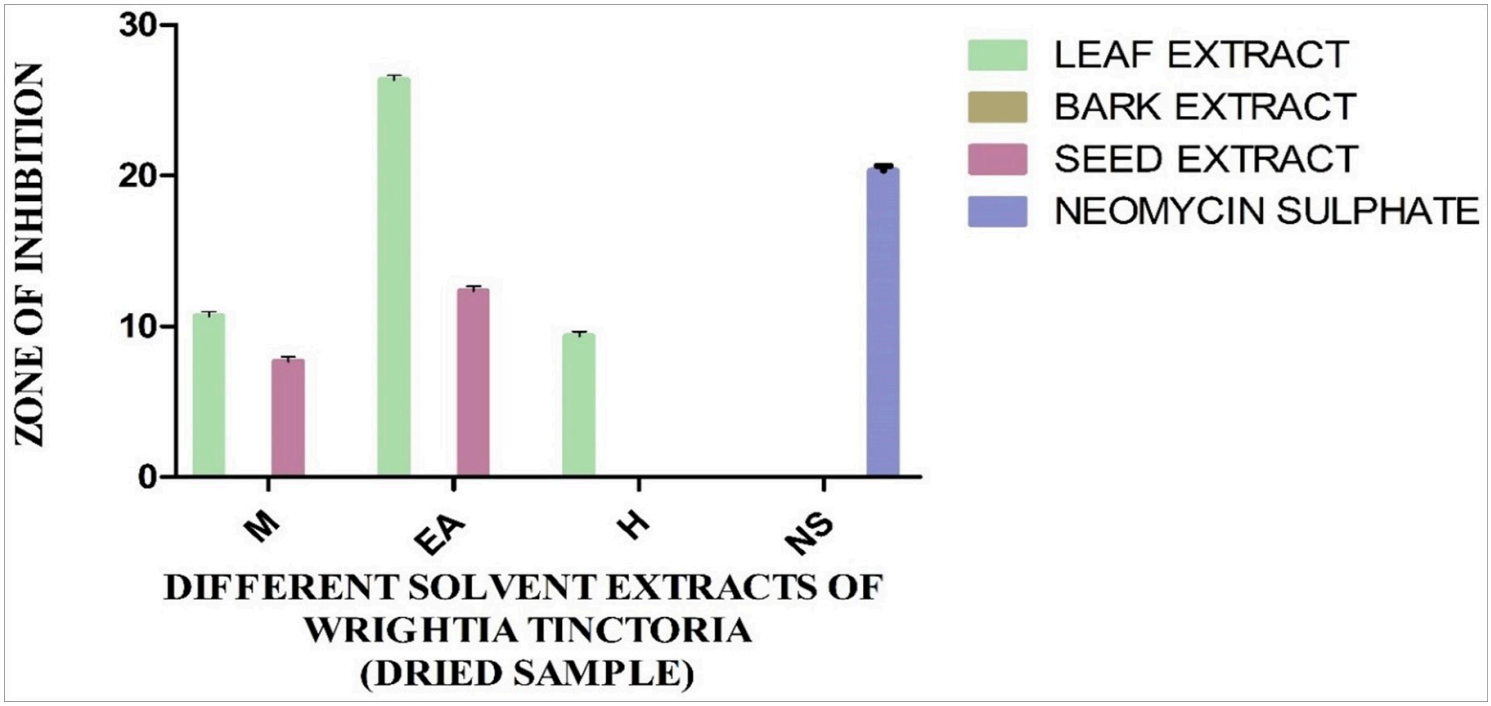

Figure 9

Figure 8. Graphical representation of antibacterial activity of *Wrightia tinctoria* (dry extract: leaf, bark, seed) on *Staphylococcus aureus*

Note: The error bar, denoting a significance level of (P ≤ 0.05), represent the standard error of the mean value. M denotes methanol, E- Ethyl acetate, H- n-Hexane and NS- neomycin sulphate

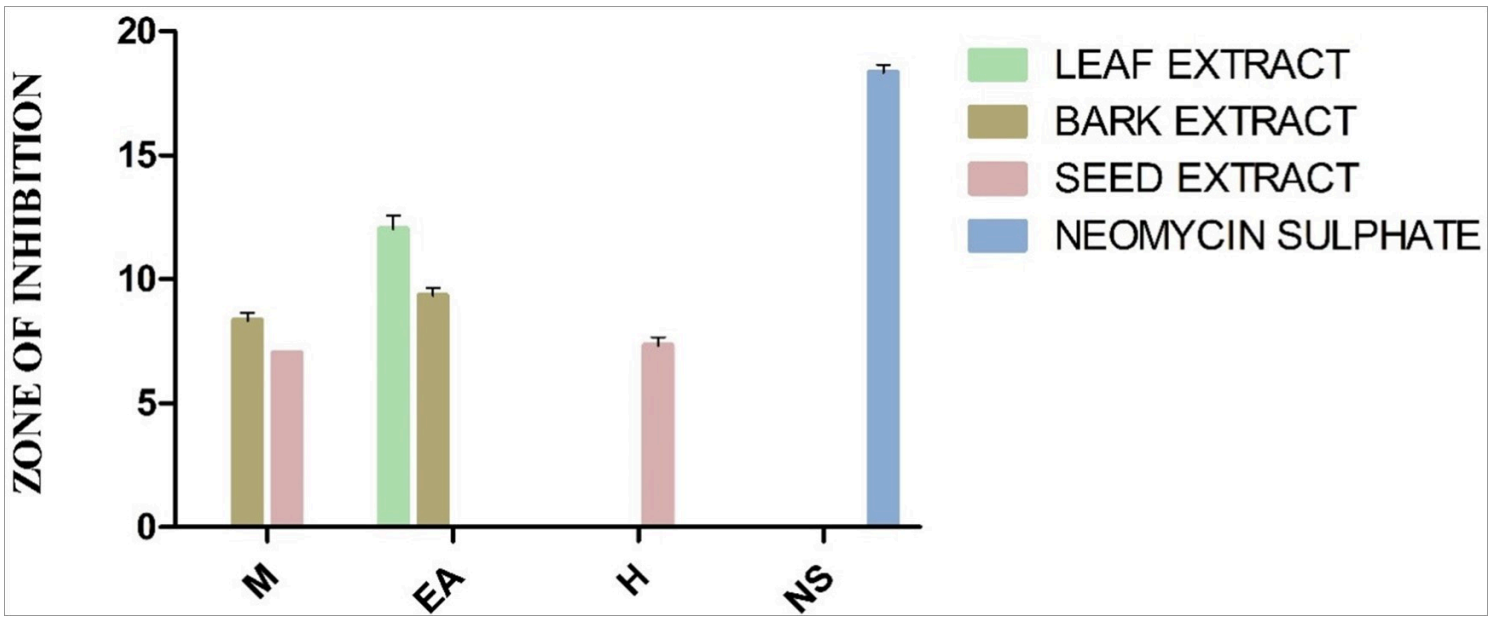

Figure 10

Figure 9. Graphical representation of antibacterial activity of *Wrightia tinctoria* (fresh extract: leaf, bark, seed) on *Staphylococcus aureus*

Note: The error bar, denoting a significance level of (P ≤ 0.05), represent the standard error of the mean value. M denotes methanol, E- Ethyl acetate, H- n-Hexane and NS- neomycin sulphate

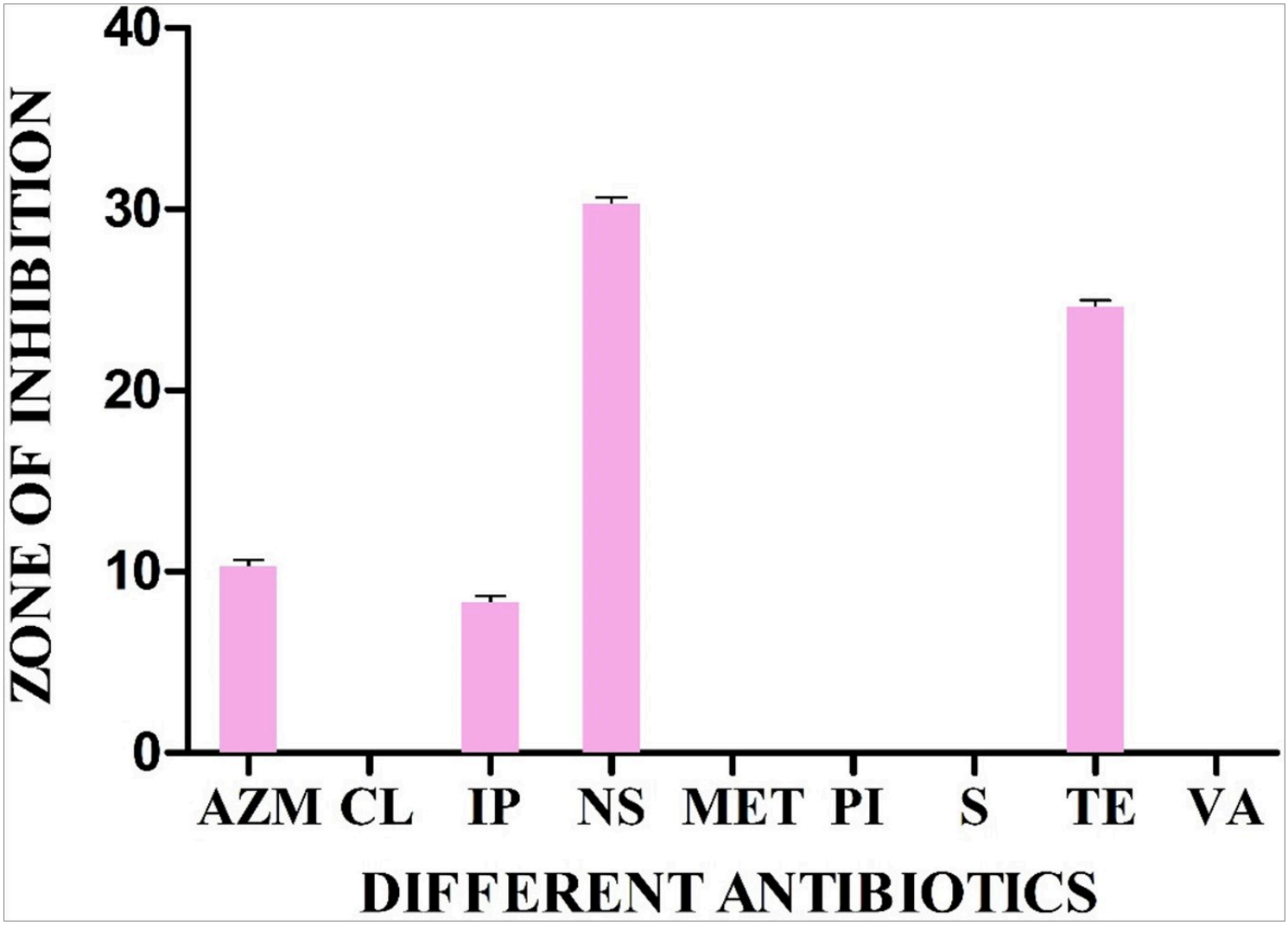

Figure 11

Figure 10. Antibiotic susceptibility Profile on *Staphylococcus aureus* to a range of commercially available antibiotics

Note: AZM denotes azithromycin, CL- colistin, IP – imipenem, NS- Neomycin Sulphate, MET- Methicillin, PI- Piperacillin, S- streptomycin, TE- Tetracycline, VA- vancomycin. The error bar, with a significance level of P ≤ 0.05, represent the standard error of the mean value.

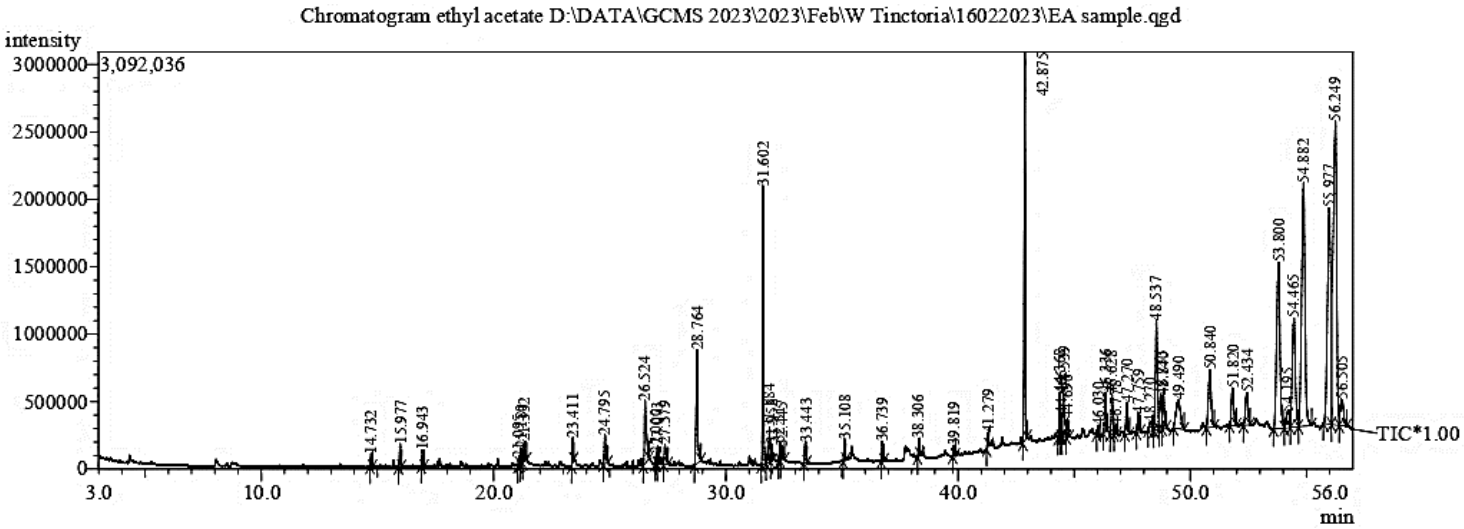

Figure 12

Figure 11. GC MS Chromatogram of ethyl acetate leaf extract of *Wrightia tinctoria*

Supplementary Files

This is a list of supplementary files associated with this preprint. Click to download.

- Supplementaryfile.docx
- Table1.docx